Acta Crystallographica Section F
Structural Biology and Crystallization Communications
ISSN 1744-3091

Improvement of the quality of lumazine synthase crystals by protein engineering

Lidia Rodríguez-Fernández,[a] F. Javier López-Jaramillo,[b] Adelbert Bacher,[a] Markus Fischer[c] and Sevil Weinkauf[a]*

[a]Department of Chemistry, Technische Universität München, Lichtenbergstrasse 4, 85747 Garching, Germany, [b]Institute of Biotechnology, Department of Organic Chemistry, University of Granada, Campus Fuentenueva, 18071 Granada, Spain, and [c]Institute of Biochemistry and Food Chemistry, University of Hamburg, Grindelallee 117, 20146 Hamburg, Germany

Correspondence e-mail: sevil.weinkauf@ch.tum.de

Received 21 April 2008
Accepted 25 May 2008

Icosahedral macromolecules have a wide spectrum of potential nanotechnological applications, the success of which relies on the level of accuracy at which the molecular structure is known. Lumazine synthase from *Bacillus subtilis* forms a 150 Å icosahedral capsid consisting of 60 subunits and crystallizes in space group $P6_322$ or $C2$. However, the quality of these crystals is poor and structural information is only available at 2.4 Å resolution. As classical strategies for growing better diffracting crystals have so far failed, protein engineering has been employed in order to improve the overexpression and purification of the molecule as well as to obtain new crystal forms. Two cysteines were replaced to bypass misfolding problems and a charged surface residue was replaced to force different molecular packings. The mutant protein crystallizes in space group $R3$, with unit-cell parameters $a = b = 313.02$, $c = 365.77$ Å, $\alpha = \beta = 90.0$, $\gamma = 120^\circ$, and diffracts to 1.6 Å resolution.

1. Introduction

Riboflavin (vitamin B_2), the universal precursor of flavocoenzymes, is essential for life and plays a crucial role in many biological processes. The enzyme lumazine synthase catalyses the penultimate step in the biosynthesis of riboflavin (Volk & Bacher, 1988). The secondary and tertiary structures of lumazine synthases from different organisms are well conserved; however, their quaternary structures differ. They exist as pentamers (Persson *et al.*, 1999; Meining *et al.*, 2000; Gerhardt *et al.*, 2002; Morgunova *et al.*, 2005, 2007), decamers (dimers of pentamers; Klinke *et al.*, 2005) and as icosahedral capsids with 60 subunits (dodecamers of pentamers; Ritsert *et al.*, 1995; Persson *et al.*, 1999; Zhang *et al.*, 2001). The icosahedral representatives are attractive models as virus-like particles with a panoply of potential applications in nanotechnology and bionanotechnology, *e.g.* for the synthesis of nanophase iron oxide (Shenton *et al.*, 2001), for encapsulation of cargo molecules (Seebeck *et al.*, 2006) and for the design of bifunctional assemblies (Fischer *et al.*, 2001).

Among the icosahedral lumazine synthases, the structure of the bifunctional lumazine synthase/riboflavin synthase complex purified from *Bacillus subtilis* was first solved at 3.3 Å resolution using crystals of space group $P6_322$, which revealed the icosahedral arrangement of 60 lumazine synthase subunits in a capsid enclosing the trimeric riboflavin synthase (Ladenstein *et al.*, 1983, 1988). An important improvement in the diffraction resolution was achieved by the crystallization of hollow capsids which were obtained by releasing the riboflavin synthase *via* dissociation of the complex and by ligand-driven reconstitution of the icosahedral capsid (Bacher *et al.*, 1986). Reconstituted hollow capsids formed hexagonal ($P6_322$) and monoclinic ($C2$) crystals (Schott *et al.*, 1990). Whereas the diffraction patterns of the hexagonal $P6_322$ crystals were characterized by strong and highly structured diffuse scattering extending to high resolution as a result of static disorder and/or internal motion, the crystals of space group $C2$ yielded data at 2.4 Å resolution with almost undetectable diffuse scattering (Schott *et al.*, 1990). Structure analysis using the latter data revealed the homology of the reconstituted capsid and the bifunctional complex and allowed a deeper under-

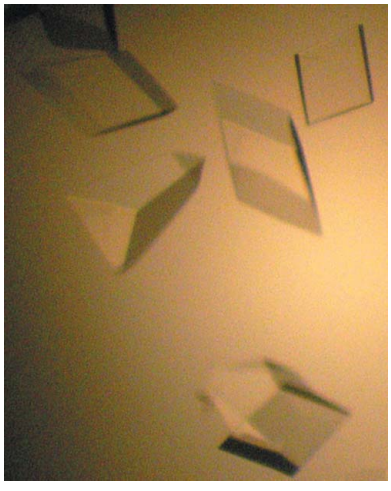

standing of the catalytic mechanism (Ritsert *et al.*, 1995). However, the facts that the active site is located on the inner wall of the capsid and that the channels are not wide enough left the questions open of how the substrates reach the active site and how the products can return to the bulk solvent.

Hollow *B. subtilis* lumazine synthase subsequently produced by recombinant methods only crystallized in space group $P6_322$ and yielded diffraction data to 2.9 Å resolution. The diffraction pattern was characterized by highly structured diffuse scattering, anisotropy and trails of reflections in one direction disclosing thermal disorder and loss of order along one of the crystallographic axes, in agreement with the significant translational and rotational disorder as visualized by electron microscopy (Braun *et al.*, 2000). Attempts to improve the diffraction properties of these crystals by common strategies, *e.g.* variation of precipitant, temperature or pH and the use of additives or diffusive environments, failed. In an attempt to better understand the possible origins of the crystal disorder and to further improve the crystal quality, we chose protein engineering as an alternative tool. Protein engineering has proven to be an efficient tool to improve the crystal quality of proteins and/or to obtain crystals of those recalcitrant to crystallization regardless of whether random mutation (McElroy *et al.*, 1992), surface-entropy reduction (Derewenda, 2004; Cooper *et al.*, 2007) or chemical modification (Schubot & Waugh, 2004; Rauert *et al.*, 2007) strategies are followed. In the case of symmetrical oligomeric proteins, however, this strategy may have severe consequences in the particle assembly (Zhang *et al.*, 2006), as the effects of even a single mutation on the protein secondary, tertiary or even quaternary structure cannot be predicted *a priori*. Nevertheless, we modified the recombinant enzyme by site-directed mutagenesis, evaluated the impact of the mutations on its quaternary structure, crystallized it and characterized the crystals by X-ray diffraction. The mutant enzyme crystallizes in space group *R*3 and diffracts X-rays to 1.6 Å resolution.

2. Materials and methods

Restriction enzymes and T4 DNA ligase were from New England Biolabs. EXT DNA Polymerase and Taq polymerase were from Finnzymes (Epsoo, Finland). Oligonucleotides were synthesized by Thermo Electron GmbH (Ulm, Germany). DNA fragments were purified with the CP-Kit, Gel Extraction Kit or Miniprep Kits from Peqlab (Erlangen, Germany) or Qiagen (Hilden, Germany).

2.1. Cloning and site-specific mutagenesis

Site-directed mutagenesis was performed using a PCR standard protocol as described elsewhere (Fischer *et al.*, 2003). Briefly, the first PCR used a pNCO113 plasmid harbouring the wild-type *ribH* gene of *B. subtilis* or a mutated version of the *ribH* gene (pNCO-BsLS-T118A, pNCO-BsLS-T118A-C93S, pNCO-BsLS-T118A-C93/139S) as template and oligonucleotide pairs M1(+E) and M3(+*X*) as primers (Table 1). The latter oligonucleotide contained a mismatch codon for the introduction of the respective mutation. The second PCR again used the starting plasmid as template and the oligonucleotide pairs M2(ΔE) and M4(+B) as primers. The amplificates from the two PCR steps were mixed and subjected to PCR without additional primers. In the final step, the reaction mixture of step 3 was re-amplified using the oligonucleotides M1(+E) and M4(+B) as primers. The amplificates were purified, digested with *Eco*RI and *Bam*HI and ligated into plasmid pNCO113, which had been treated with the same restriction enzymes. The ligation mixture was transformed into *Escherichia coli* XL1 Blue cells. Transformants were selected on LB solid medium supplemented with ampicillin (150 mg l^{-1}). After the selection plasmids had been purified and sequenced (GATC Biotech, Konstanz, Germany), the sequence of the final construct (pNCO-BsLS-D44G-C93/139S-T118A) was deposited in the GenBank sequence database (accession No. EU258474).

Table 1
Oligonucleotides used for construction of expression plasmids.

Designation	Restriction site for cloning	Sequence (5′ to 3′)
M1(+E)	*Eco*RI	AGATATTTTCATTAAAGAGGAGAA
M2(ΔE)	—	AGATATTTTCATTAAAGAGGAGAA
M4(+B)	*Bam*HI	CTGCAGGTCGACGGATCC
M3(+D44G)	—	GTCATTTGTGCCTACGCCATGTCTG
M3(+C93S)	—	GCAGCTTCATTCGAAACATAATCG
M3(+T118A)	—	CGATGTTTTCAGCTGTTACAATTC
M3(+C139S)	—	GGCAGAAACAGCTGAATCTACACC

2.2. Overexpression and purification

The protein was overexpressed in *E. coli* M15[pREP4] harbouring the plasmid pNCO-BsLS-D44G-C93/139S-T118A. Bacteria were grown aerobically in LB medium containing ampicillin (170 mg l^{-1}) and kanamycin (20 mg l^{-1}) at 310 K to an optical density at 600 nm of about 0.7 and then induced with 2 m*M* isopropyl β-D-1-thiogalactopyranoside (Bissendorf Biochemicals) for 5 h. Cells were harvested by centrifugation (Sorvall GS3 rotor, 4200*g*, 15 min, 277 K), washed twice with 0.9% NaCl and stored at 153 K. Frozen cell mass was thawed in 50 m*M* potassium phosphate pH 7.0 containing 0.5 m*M* EDTA, 0.5 m*M* sodium sulfite and 0.02% sodium azide. The suspension was cooled on ice, ultrasonically treated and centrifuged (Beckman 70 Ti rotor, 149 000*g*, 45 min, 277 K). The supernatant was loaded onto a Q-Sepharose FF (Amersham Pharmacia Biotech) column (3 × 25 cm) equilibrated with 20 m*M* potassium phosphate pH 7.0. After washing with 100 ml 20 m*M* potassium phosphate pH 7.0, the protein was eluted with a linear gradient of 0.02–1.0 *M* potassium phosphate pH 7.0 (total volume 800 ml). Fractions were checked by SDS–PAGE and those containing the recombinant protein were concentrated by ultracentrifugation (Beckman 70 Ti rotor, 18 h, 75 000*g*, 277 K). The concentrated protein was injected onto a Superdex 200 gel-filtration (Amersham Pharmacia Biotech) column (1.6 × 60 cm) and eluted with 0.1 *M* sodium/potassium phosphate pH 8.7. Fractions were concentrated to 10 mg ml^{-1} by ultracentrifugation and the substrate analogue 5-nitro-6-(D-ribitylamino)-2,4(1*H*,3*H*)-pyrimidinedione was added to a final concentration of 1 m*M*.

2.3. Crystallization

Crystallization conditions were screened by the sitting-drop vapour-diffusion method using sparse-matrix screens (Jancarik & Kim, 1991) based on Crystal Screens I and II (Hampton Research). Crystals for X-ray diffraction were grown in Cryschem plates (Hampton Research) from 10 µl droplets containing 5.4 mg ml^{-1} protein solution and 1.5 *M* ammonium sulfate in 0.2 *M* Tris–HCl pH 8.5. Evaporation of the droplet was minimized using 1 ml 1.5 *M* ammonium sulfate as reservoir.

2.4. X-ray diffraction

Data were collected on ESRF beamline BM16 using an ADSC Q210R detector placed 154 mm from a single crystal (0.4 × 0.3 × 0.4 mm; 0.048 mm^3) cryoprotected by soaking in 0.2 *M* Tris–HCl pH

Table 2
Main features of the data set.

Values in parentheses are for the highest resolution shell.

Beamline	BM16 (ESRF)
Detector	ADSC Q210R
Wavelength (Å)	0.99
Temperature (K)	100
No. of crystals	1
Space group	*R*3
Unit-cell parameters (Å, °)	$a = b = 313.02$, $c = 365.77$, $\alpha = \beta = 90$, $\gamma = 120$
Resolution range (Å)	50–1.6 (1.7–1.6)
Measured reflections	12898357
Unique reflections	1718572
$R_{\rm merge}$ (%)	11.4 (53.8)
Completeness (%)	97.5 (86.4)
Completeness [$I/\sigma(I) > 2$] (%)	88.0 (60.6)
Mean $I/\sigma(I)$	11.64 (3.22)

8.5, 1.5 *M* ammonium sulfate and increasing concentrations of glycerol up to 12%(*v*/*v*). The oscillation angle was 0.25° and the exposure time was 30 s per frame. Data were processed with the *XDS* software package (Kabsch, 1988, 1993) following a forward-directed search strategy (Kabsch, 1993). The reduced cell was determined without imposing symmetry or unit-cell parameters and the resulting cell was compared with all 44 possible lattices and indexed in *P*1. Diffraction parameters and the unit cell were refined in *R*3, the space group with the highest likelihood of being correct according to *XDS*, and the data set was re-indexed in *R*3 and scaled with *XSCALE*. Overloads and incomplete reflections, *i.e.* reflections with an intensity estimate at profile fitting of less than 75% of the observed intensity, were rejected. Based on the Matthews probability calculator (Kantardjieff & Rupp, 2003) and the internal symmetry of the capsid, the $V_{\rm M}$ was estimated as 2.59 Å^3 Da^{-1}, which corresponds to 16 pentamers per asymmetric unit.

3. Results and discussion

In the case of recombinant *B. subtilis* lumazine synthase, all common strategies for the growth of high-quality crystals have failed, leaving protein engineering as the only alternative tool. We started with the lumazine synthase variant Thr118Ala, which was produced in the course of our earlier studies on the reaction mechanism of lumazine synthase, and replaced three further amino-acid residues. We mutated the cysteines 93 and 139 to serines in order to obtain a cysteine-free molecule and to bypass misfolding problems. Cys93 located at the α3-helix at the central channel of the pentameric ring can be replaced without changes in the quaternary structure even if distortions in the secondary structure are induced (Woycechowsky *et al.*, 2006). Cys139 is part of the α4 helix which is not crucial for the icosahedral assembly (Fornasari *et al.*, 2004; Zhang *et al.*, 2001). The fourth mutation was targeted on Asp44, which is located at the surface of the capsid and is involved in crystal contacts in both the *C*2 and $P6_322$ crystal forms (unpublished data). By the replacement of Asp44 by Gly, we aimed at the distortion of the abovementioned lumazine synthase crystal lattices that are already known to yield low-resolution data sets, increasing the likelihood of crystals with different symmetry.

The integrity of the fourfold-mutated enzyme was confirmed by size-exclusion chromatography and electron microscopy. The protein eluted from the Superdex 200 gel-filtration column with a retention time comparable to that of the wild-type enzyme complex. Electron-microscopic analysis of negatively stained samples revealed particles with a morphology and a size resembling the $T = 1$ icosahedral capsids (Fig. 1).

Crystallization screenings led to microcrystals of the mutant enzyme under several conditions, with ammonium sulfate and ammonium phosphate turning out to be the most effective precipitants for growing large single crystals. Despite the similarity of the crystallization conditions, crystals of the engineered enzyme devel-

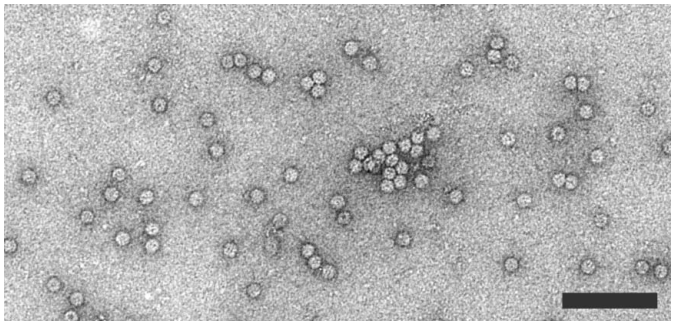

Figure 1
Transmission electron micrograph of the mutant lumazine synthase negatively stained with uranyl acetate [1%(*w*/*v*); pH 4.6]. The scale bar represents 100 nm.

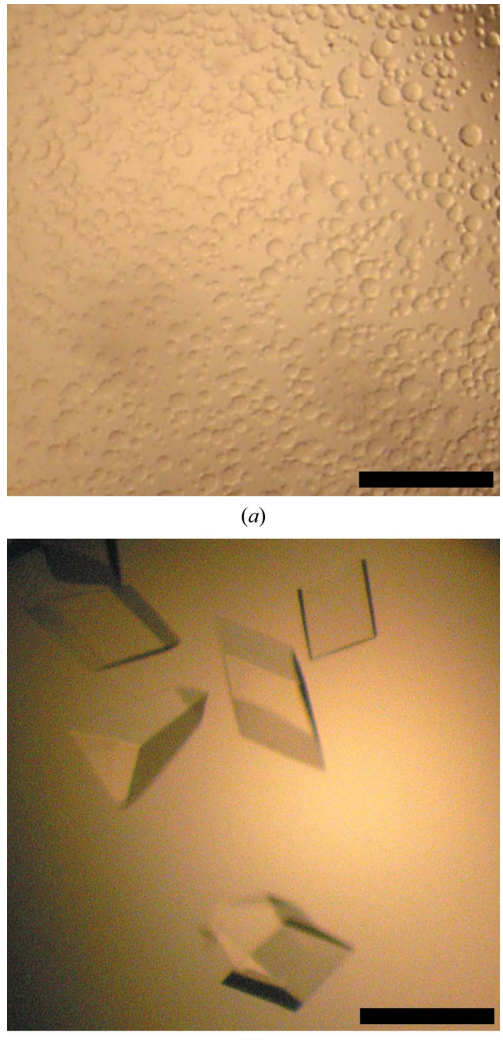

(*a*)

(*b*)

Figure 2
(*a*) Liquid–liquid phase separation observed in crystallization drops that led to crystals after 5 d (*b*). The scale bar represents 500 µm.

oped from a visible liquid–liquid phase separation in contrast to the wild-type protein (Fig. 2; Gliko *et al.*, 2005).

Preliminary crystallographic analysis revealed that the mutant enzyme crystallized in space group *R*3, suggesting contacts in the crystal lattice that are rather different than those in the *C*2 and $P6_322$ space groups. Based on the Matthews probability calculator and the internal symmetry of the capsid, the V_M was estimated as 2.59 $Å^3\ Da^{-1}$, which corresponds to 16 pentamers per asymmetric unit. The diffraction pattern was characterized by the absence of structured diffuse scattering or anisotropic features compared with the wild-type protein. Diffraction of a 0.4 × 0.3 × 0.4 mm crystal (0.048 mm^3) yielded the data set summarized in Table 2 and confirmed the success of our approach. The resolution extended to 1.6 Å, which is the best resolution ever achieved for lumazine synthase from *B. subtilis* and is on a par with the resolution obtained with the enzyme from the hyperthermophilic eubacterium *Aquifex aeolicus* (Zhang *et al.*, 2001). Work is currently in progress towards structure determination by molecular replacement and towards analysis of the crystal rotational order by transmission electron microscopy.

This work was supported by a grant from Bundesministerium für Bildung und Forschung (50WB0012) to SW and a grant from 'Programa de Retorno de Investigadores a Centros de Investigación y Universidades de Andalucía' (Junta de Andalucia, Spain) to FJLJ. Diffraction at BM16 (ESRF) was carried out in the frame of the project MX-578 funded by the European Community Research Infrastructure Action under the FP6 'Structuring the European Research Area Programme' (contract No. RII3-CT-2004-506008). We are grateful to the BM16 staff A. Labrador and G. Fox for excellent assistance during data collection and to B. Illarionov for his assistance in plasmid isolation. FJLJ is indebted to F. Santoyo, A. Osuna and P. Aranda for their support.

References

Bacher, A., Ludwig, H. C., Schnepple, H. & Ben-Shaul, Y. (1986). *J. Mol. Biol.* **187**, 75–86.
Braun, N., Tack, J., Fischer, M., Bacher, A., Bachmann, L. & Weinkauf, S. (2000). *J. Cryst. Growth*, **212**, 270–282.
Cooper, D. R., Boczek, T., Grelewska, K., Pinkowska, M., Sikorska, M., Zawadzki, M. & Derewenda, Z. (2007). *Acta Cryst.* D**63**, 636–645.
Derewenda, Z. S. (2004). *Structure*, **12**, 529–535.
Fischer, M., Bacher, A., Haase, I., Tristl, M. & Sackmann, E. (2001). *Chem. Phys. Chem.* **10**, 623–627.
Fischer, M., Haase, I., Kis, K., Meining, W., Ladenstein, R., Cushman, M., Schramek, N., Huber, R. & Bacher, A. (2003). *J. Mol. Biol.* **326**, 783–793.
Fornasari, M. S., Laplagne, D. A., Frankel, N., Cauerhoff, A. A., Goldbaum, F. A. & Echave, J. (2004). *Mol. Biol. Evol.* **21**, 97–107.
Gerhardt, S., Haase, I., Steinbacher, S., Kaiser, J. T., Cushman, M., Bacher, A., Huber, R. & Fischer, M. (2002). *J. Mol. Biol.* **318**, 1317–1329.
Gliko, O., Neumaier, N., Pan, W., Haase, I., Fischer, M., Bacher, A., Weinkauf, S. & Vekilov, P. G. (2005). *J. Cryst. Growth*, **275**, 1409–1416.
Jancarik, J. & Kim, S.-H. (1991). *J. Appl. Cryst.* **24**, 409–411.
Kabsch, W. (1988). *J. Appl. Cryst.* **21**, 916–924.
Kabsch, W. (1993). *J. Appl. Cryst.* **26**, 795–800.
Kantardjieff, K. & Rupp, B. (2003). *Protein Sci.* **12**, 1865–1871.
Klinke, S., Zylberman, V., Vega, D. R., Guimaraes, G., Braden, B. C. & Goldbaum, F. A. (2005). *J. Mol. Biol.* **353**, 124–137.
Ladenstein, R., Ludwig, H. C. & Bacher, A. (1983). *J. Biol. Chem.* **258**, 11981–11983.
Ladenstein, R., Scheider, M., Huber, R., Bartunik, H. D., Wilson, K., Schott, K. & Bacher, A. (1988). *J. Mol. Biol.* **203**, 1045–1070.
McElroy, H. H., Sisson, G. W., Schottlin, W. E., Aust, R. M. & Villafranca, J. E. (1992). *J. Cryst. Growth*, **122**, 265–272.
Meining, W., Mörtl, S., Fischer, M., Cushman, M., Bacher, A. & Ladenstein, R. (2000). *J. Mol. Biol.* **299**, 181–197.
Morgunova, E., Meining, W., Illarionov, B., Haase, I., Jin, G., Bacher, A., Cushman, M., Fischer, M. & Ladenstein, R. (2005). *Biochemistry*, **44**, 2746–2758.
Morgunova, E., Saller, S., Haase, I., Cushman, M., Bacher, A., Fischer, M. & Ladenstein, R. (2007). *J. Biol. Chem.* **282,** 17231–17241.
Persson, K., Schneider, G., Jordan, D. B., Viitanen, P. V. & Sandalova, T. (1999). *Protein Sci.* **8**, 2355–2365.
Rauert, W., Eddine, A. N., Kaufmann, S. H. E., Weiss, M. S. & Janowski, R. (2007). *Acta Cryst.* F**63**, 507–511.
Ritsert, K., Huber, R., Turk, D., Ladenstein, R., Schmidt-Base, K. & Bacher, A. (1995). *J. Mol. Biol.* **253**, 151–167.
Schott, K., Ladenstein, R., Konig, A. & Bacher, A. (1990). *J. Biol. Chem.* **265**, 12686–12689.
Schubot, F. D. & Waugh, D. S. (2004). *Acta Cryst.* D**60**, 1981–1986.
Seebeck, F. P., Woycechowsky, K. J., Zhuang, W., Rabe, J. P. & Hilvert, D. (2006). *J. Am. Chem. Soc.* **128**, 4516–4517.
Shenton, W., Mann, S., Colfen, H., Bacher, A. & Fischer, M. (2001). *Angew. Chem. Int. Ed.* **40**, 442–445.
Volk, R. & Bacher, A. (1988). *J. Am. Chem. Soc.* **110**, 3651–3653.
Woycechowsky, K. J., Seebeck, F. P. & Hilvert, D. (2006). *Protein Sci.* **15**, 1106–1114.
Zhang, X., Konarev, P. V., Petoukhov, M. V., Svergun, D. I., Xing, L., Cheng, H., Haase, I., Fischer, M., Bacher, A., Ladenstein, R. & Meining, W. (2006). *J. Mol. Biol.* **362**, 753–770.
Zhang, X., Meining, W., Fischer, M., Bacher, A. & Ladenstein, R. (2001). *J. Mol. Biol.* **306**, 1099–1114.